

# Numerical analysis of the rebellious voter model

Jan M. Swart\*

Karel Vrbenský \*

November 6, 2009

## Abstract

The rebellious voter model, introduced by Sturm and Swart (2008), is a variation of the standard, one-dimensional voter model, in which types that are locally in the minority have an advantage. It is related, both through duality and through the evolution of its interfaces, to a system of branching annihilating random walks that is believed to belong to the ‘parity-conservation’ universality class. This paper presents numerical data for the rebellious voter model and for a closely related one-sided version of the model. Both models appear to exhibit a phase transition between noncoexistence and coexistence as the advantage for minority types is increased. For the one-sided model (but not for the original, two-sided rebellious voter model), it appears that the critical point is exactly a half and two important functions of the process are given by simple, explicit formulas, a fact for which we have no explanation.

*MSC 2000.* Primary: 82C22; Secondary: 65C05, 82C26, 60K35

*Keywords.* Rebellious voter model, parity conservation, exactly solvable model, coexistence, interface tightness, cancellative systems, Markov chain Monte Carlo.

*Acknowledgements.* Work sponsored by GAČR grant 201/06/1323 and MŠMT ČR grant DAR 1M0572.

## Contents

<b>1</b>	<b>Introduction</b>	<b>2</b>
1.1	Definition of the models . . . . .	2
1.2	Interface and dual models . . . . .	3
1.3	Coexistence, survival and interface tightness . . . . .	4
1.4	Known results . . . . .	5
<b>2</b>	<b>Main results</b>	<b>7</b>
2.1	Methods . . . . .	7
2.2	A first qualitative look . . . . .	8
2.3	The two-sided model . . . . .	9
2.4	The one-sided model . . . . .	11
2.5	Finite size effects . . . . .	12
<b>3</b>	<b>Other functions of the process</b>	<b>15</b>
3.1	Harmonic functions . . . . .	15
3.2	Frequencies for three and more particles . . . . .	18
3.3	Edge speeds . . . . .	20

---

\*swart@utia.cas.cz and vrbensky@utia.cas.cz, Institute of Information Theory and Automation of the ASCR (ÚTIA), Pod vodárenskou věží 4, 18208 Praha 8, Czech Republic. URL <http://staff.utia.cas.cz/swart/>

# 1 Introduction

## 1.1 Definition of the models

Let

$$\{0, 1\}^{\mathbb{Z}} := \{x = (x(i))_{i \in \mathbb{Z}} : x(i) \in \{0, 1\} \forall i \in \mathbb{Z}\} \quad (1.1)$$

be the space whose elements  $x$  are infinite arrays of zeroes and ones, situated on the integer lattice  $\mathbb{Z}$ . We will be interested in Markov processes taking values in  $\{0, 1\}^{\mathbb{Z}}$ . More precisely, we study the *rebellious voter model* introduced in [SS08a], and a variation on this model, which we call the *one-sided rebellious voter model*. For expository reasons, we will also shortly discuss two other models, the *disagreement* and *swapping voter models*.

In the one-sided rebellious voter model, initially, each site  $i \in \mathbb{Z}$  has a type  $x(i) \in \{0, 1\}$  assigned to it, and these types are updated according to the following stochastic dynamics. Independently for each site  $i \in \mathbb{Z}$ , one constructs times  $0 < \tau_1(i) < \tau_2(i) < \dots$  according to a Poisson process with rate 1, i.e.,  $\tau_1(i) - 0, \tau_2(i) - \tau_1(i), \tau_3(i) - \tau_2(i), \dots$  are i.i.d. exponentially distributed with mean 1. At each time  $t = \tau_k(i)$ , with  $k = 1, 2, \dots$ , the type of site  $i$  is updated according to the following rules. With probability  $\alpha$ , the site  $i$  looks at the site  $i - 1$  on its left, and if the type of site  $i - 1$  is different from the type of  $i$ , then site  $i$  changes its type. With the remaining probability  $1 - \alpha$ , the site  $i$  looks at the two sites  $i - 2$  and  $i - 1$  on its left, and if the type of site  $i - 2$  is different from the type of  $i - 1$ , then site  $i$  changes its type. If we let  $X_t(i)$  denote the type of site  $i$  at time  $t$ , then  $(X_t)_{t \geq 0}$  is a continuous-time Markov process taking values in  $\{0, 1\}^{\mathbb{Z}}$ , which we call the *one-sided rebellious voter model*. Another way of describing its dynamics is to say that in this model, for any  $i \in \mathbb{Z}$ , the process  $X$  makes the transition

$$\begin{aligned} x \mapsto x^{\{i\}} \quad \text{with rate} \\ \alpha 1_{\{x(i-1) \neq x(i)\}} + (1 - \alpha) 1_{\{x(i-2) \neq x(i-1)\}}, \end{aligned} \quad (1.2)$$

where  $1_A$  denotes the indicator function of an event  $A$  and for any  $x \in \{0, 1\}^{\mathbb{Z}}$  and  $\Delta \subset \mathbb{Z}$ , we let

$$x^{\Delta}(j) := \begin{cases} 1 - x(j) & \text{if } j \in \Delta, \\ x(j) & \text{if } j \notin \Delta \end{cases} \quad (1.3)$$

denote the configuration obtained from  $x$  by changing the types of all sites in  $\Delta$ .

The original *rebellious voter model* as introduced in [SS08a] is similar to the process described above, except that sites do not only look to the left, but also to the right when deciding whether to update their type. More precisely, in this case, at each time  $\tau_k(i)$  as defined above, the site  $i$  decides, with probability  $1/2$  each, to look either to the left or to the right. If the site looks to the left, then its type is updated as before. If the site  $i$  looks to the right, then with probability  $\alpha$ , it looks at the site  $i + 1$  on its right, and if the types of  $i$  and  $i + 1$  are different, then  $i$  changes its type. With the remaining probability  $1 - \alpha$ , the site  $i$  looks at the two sites  $i + 1$  and  $i + 2$  on its right, and if the types of  $i + 1$  and  $i + 2$  differ from each other, then  $i$  changes its type. Another way of describing these dynamics is to say that in this model, for any  $i \in \mathbb{Z}$ , the process makes the transition

$$\begin{aligned} x \mapsto x^{\{i\}} \quad \text{with rate} \\ \frac{1}{2} \alpha (1_{\{x(i-1) \neq x(i)\}} + 1_{\{x(i) \neq x(i+1)\}}) \\ + \frac{1}{2} (1 - \alpha) (1_{\{x(i-2) \neq x(i-1)\}} + 1_{\{x(i+1) \neq x(i+2)\}}). \end{aligned} \quad (1.4)$$

We note that our description of the rebellious voter model differs a factor  $1/2$  in the speed of time in comparison to the original definition in [SS08a].

A third and fourth model, that we also shortly discuss in this introduction, are the *disagreement* and *swapping voter models*. The disagreement voter model evolves as

$$\begin{aligned} x \mapsto x^{\{i\}} & \text{ with rate} \\ & \alpha(1_{\{x(i-1) \neq x(i)\}} + 1_{\{x(i) \neq x(i+1)\}}) + (1 - \alpha)1_{\{x(i-1) \neq x(i+1)\}}, \end{aligned} \quad (1.5)$$

while the swapping voter model evolves as

$$\begin{aligned} x \mapsto x^{\{i\}} & \text{ with rate} & \alpha(1_{\{x(i-1) \neq x(i)\}} + 1_{\{x(i) \neq x(i+1)\}}), \\ x \mapsto x^{\{i,i+1\}} & \text{ with rate} & (1 - \alpha)1_{\{x(i) \neq x(i+1)\}}. \end{aligned} \quad (1.6)$$

In case of the rebellious voter model and its one-sided counterpart, the parameter  $0 \leq \alpha \leq 1$  can be interpreted as the *competition parameter*. For  $\alpha = 1$ , the model is a standard, one-dimensional voter model, as first introduced in [CS73, HL75]. For  $\alpha < 1$ , one can check that the dynamics give an advantage to types that are locally in the minority. As a consequence, at least on a heuristic level, decreasing  $\alpha$  should make it harder for any type to die out. The rebellious voter model has been introduced in [SS08a] in an attempt to model the distribution of two closely related species where competition between organisms belonging to different species is less strong than competition between organisms of the same species.

## 1.2 Interface and dual models

The models introduced so far are in two ways related to parity preserving branching annihilating particle systems. First, if  $X$  is any of the models defined in (1.2) and (1.4)–(1.6), then setting

$$Y_t(i) := 1_{\{X_t(i) \neq X_t(i+1)\}} \quad (t \geq 0, i \in \mathbb{Z}) \quad (1.7)$$

defines a Markov process taking values in  $\{0, 1\}^{\mathbb{Z}}$  that we call the *interface model* associated with  $X$ . (The sites  $i$  such that  $X_t(i) \neq X_t(i+1)$  are called interfaces, or also *kinks* or *domain walls*.) Indeed, in case of the one-sided rebellious voter model, it is not hard to see that  $Y$  jumps as

$$y \mapsto y^{\{i,i+1\}} \text{ with rate } \alpha 1_{\{y(i)=1\}} + (1 - \alpha)1_{\{y(i-1)=1\}}, \quad (1.8)$$

where we use notation defined in (1.3). For the two-sided process, the dynamics of  $Y$  are given by

$$\begin{aligned} y \mapsto y^{\{i,i+1\}} & \text{ with rate} \\ & \frac{1}{2}\alpha(1_{\{y(i)=1\}} + 1_{\{y(i+1)=1\}}) + \frac{1}{2}(1 - \alpha)(1_{\{y(i-1)=1\}} + 1_{\{y(i+2)=1\}}) \end{aligned} \quad (1.9)$$

(see [SS08a, Section 1.2]), while for the disagreement voter model we get the ‘swapping annihilating random walk’ (SARW)

$$y \mapsto y^{\{i,i+1\}} \text{ with rate } \alpha(1_{\{y(i)=1\}} + 1_{\{y(i+1)=1\}}) + (1 - \alpha)1_{\{y(i) \neq y(i+1)\}}, \quad (1.10)$$

and for swapping voter model we get

$$\begin{aligned} y \mapsto y^{\{i,i+1\}} & \text{ with rate} & \alpha(1_{\{y(i)=1\}} + 1_{\{y(i+1)=1\}}) \\ y \mapsto y^{\{i-1,i+1\}} & \text{ with rate} & (1 - \alpha)1_{\{y(i)=1\}}. \end{aligned} \quad (1.11)$$

Following [Sud90], we call this latter model the double branching annihilating random walk (DBARW); very similar models (usually in discrete time) have been called BARW2 or BAW in the physics literature (see, e.g., [TT92]).

In each of these interface models, since  $Y$  always flips the types of two sites at once, it is easy to see that  $Y$  *preserves parity*, i.e., if  $Y$  is started in an initial state  $Y_0$  which contains a finite, even (resp. odd) number of ones, then  $Y_t$  contains an even (resp. odd) number of ones for each  $t \geq 0$ . In particular, if  $Y$  is started with an odd number of ones, then the ones can never completely die out.

There is a second relation between our models and parity preserving branching-annihilating particle systems, namely, through duality. Let  $xy(i) := x(i)y(i)$  denotes the componentwise product of configurations  $x, y \in \{0, 1\}^{\mathbb{Z}}$ , and let  $|z| := \sum_i z(i)$  denote the number of ones in a configuration  $z$ . Then, since our models are cancellative particle systems in the sense of [Gri79], for each of our processes  $X$  there exists a dual Markov process  $Y$  whose transition probabilities are uniquely determined by the requirement that

$$\mathbb{P}[|X_t Y_0| \text{ is odd}] = \mathbb{P}[|X_0 Y_t| \text{ is odd}] \quad (t \geq 0) \quad (1.12)$$

whenever  $X$  and  $Y$  are independent (with arbitrary initial laws), and either  $|X_0|$  or  $|Y_0|$  is finite.

A special property of the rebellious voter model (that motivated its introduction in [SS08a]) is that its interface model and dual model coincide, i.e., if  $X$  is the rebellious voter model, then (1.12) holds for the same  $Y$ , with dynamics described in (1.9), that also describes the interfaces of  $X$  (see [SS08a, formula (1.8)]). For the one-sided rebellious voter model, this is not quite the case; however, its dual is the mirror image of its interface model, i.e., its dual is the model with dynamics described by (compare (1.8))

$$y \mapsto y^{\{i-1, i\}} \quad \text{with rate} \quad \alpha 1_{\{y(i)=1\}} + (1 - \alpha) 1_{\{y(i+1)=1\}}. \quad (1.13)$$

It turns out that the dual of the disagreement model is the DBARW (which is the interface model of the swapping voter model) while the dual of the swapping voter model is the SARW (which is the interface model of the disagreement voter model) (see [SS08a, Section 2.1]). Note that in the SARW there is no branching, which has far-reaching consequences for both the disagreement and swapping voter models.

### 1.3 Coexistence, survival and interface tightness

It is easy to see that the constant configurations  $\underline{0}$  and  $\underline{1}$  are traps for the various voter models we have introduced. By definition, we say that a Markov process taking values in  $\{0, 1\}^{\mathbb{Z}^d}$  exhibits *coexistence* if there exists an invariant law that is concentrated on configurations that are not identically zero or one. It is known that nearest-neighbor voter models on  $\mathbb{Z}^d$  exhibit coexistence if and only if  $d > 2$ ; in particular, for  $\alpha = 1$ , our models, being one-dimensional voter models, do not exhibit coexistence. On the other hand, our models exhibit coexistence for  $\alpha = 0$  since in this case one can check that product measure with intensity a half is an invariant law.

The question is whether there is a nontrivial phase transition between coexistence and noncoexistence. For the disagreement and swapping voter models it turns out that this is not the case. Indeed, it can be rigorously proved [Sud90, NP99, SS08a] that these model exhibits noncoexistence for all  $\alpha > 0$ . On the other hand, it appears that the rebellious voter model

and its one-sided counterpart do exhibit a nontrivial phase transition between coexistence and noncoexistence at some  $0 < \alpha_c < 1$ .

We will mainly be interested in two functions of our processes. It is said that a voter model *survives* if there is a positive probability that the process started with a single one never gets trapped in  $\underline{0}$ . In view of this, for the (one- or two-sided) rebellious voter model with competition parameter  $\alpha$ , we will be interested in the *survival probability*

$$\rho(\alpha) := \mathbb{P}^{\delta_0} [X_t \neq \underline{0} \ \forall t \geq 0], \quad (1.14)$$

where  $\mathbb{P}^{\delta_0}$  denotes the law of the process started in  $X_0 = \delta_0$ , with  $\delta_0(i) := 1_{\{i=0\}}$ . It seems plausible that for many models of the type we are considering, survival is equivalent to coexistence. Indeed, using the fact that its interface and dual models coincide, this can be rigorously proved for the rebellious voter model [SS08a, Lemma 2]; the same proof works for the one-sided process. One of the main aims of the present paper is to obtain good numerical data for the function  $\rho$ .

The function  $\rho$  quantifies, in a sense, how strongly the process exhibits coexistence (see also formulas (1.7) and (2.1) below). We need a similar formula to quantify noncoexistence. For any  $i \in \mathbb{Z}$ , let  $x_i^H \in \{0, 1\}^{\mathbb{Z}}$ , defined as

$$x_i^H(j) := \begin{cases} 0 & \text{if } j < i, \\ 1 & \text{if } i \leq j \end{cases} \quad (1.15)$$

denote a ‘Heaviside’ configuration of zeros and ones that are ‘completely separated’. Following [CD95], we say that a model  $X$  (with given parameter  $\alpha$ ) exhibits *interface tightness* if

$$\chi(\alpha) := \lim_{t \rightarrow \infty} \mathbb{P}^{x_0^H} [X_t = x_i^H \text{ for some } i \in \mathbb{Z}] > 0, \quad (1.16)$$

i.e., if the process started in a Heaviside configuration spends a positive fraction of its time in such configurations. It is intuitively plausible that interface tightness implies noncoexistence. It is rigorously known that the swapping voter model exhibits interface tightness for all  $\alpha > 0$  [SS08b].

The main aim of the present paper is to obtain good numerical data for the functions  $\rho$  and  $\chi$ , both for the rebellious voter model and for its one-sided analogue.

## 1.4 Known results

The study of parity preserving branching-annihilating particle systems has a long history in the physics literature. Their main interest lies in the fact that they provide a rare example of systems that exhibit a phase transition of survival/extinction type (the physics literature usually speaks of a transition between an ‘active’ and an ‘absorbing’ phase) that does not belong to the directed percolation (DP) universality class.

Indeed, the phase transition of these models appears to belong to a different ‘parity conservation’ (PC) universality class, characterized by its own critical exponents. The first example of a phase transition belonging to this universality class was described in [GKT84]; this concerned a one-dimensional model for interfaces, motivated by solid state physics. Numerical simulations for parity preserving branching-annihilating particle systems on  $\mathbb{Z}^d$  in dimensions  $d = 1, 2, 3$  and also on Sierpinski gaskets can be found in [TT92]. Further simulations for a one-dimensional model were made in [Jen94]. This paper also contains the conjecture that the order parameter critical exponent  $\beta$  equals  $13/14$ ; in another paper the author has conjectured

that  $\beta = 1$ . The latter value was also found in [IT98], while more recent literature seems to agree on a value of  $\beta \approx 0.92$  or slightly higher, see e.g. [Hin00, OS05]. Our work is relevant to the question of determining the value of  $\beta$  since our proposed explicit formula for the survival probability  $\rho$  of the one-sided rebellious voter model, if it is correct, implies that  $\beta = 1$ .

Field-theoretic (renormalization group) work on the PC universality class was carried out in [CT98], who found two critical dimensions. The (usual) upper critical dimension is  $d_c = 2$ , above which one should find mean-field exponents. There is, however, a second critical dimension  $d'_c \approx 4/3$  (the literature is unclear as to whether this is an exact or approximate value) such that only in dimensions below  $d'_c$  there is a nontrivial absorbing phase. Except for field-theoretical arguments, it seems no reasons have been suggested in the literature explaining the origin of this second critical dimension.

We suggest the following possible explanation. Consider three independent random walks started from some arbitrary but fixed initial positions, and let  $\tau_{ij}$  be the first time the  $i$ -th and  $j$ -th walk meet. In dimensions  $d < 2$ , it seems plausible that

$$\mathbb{P}[\tau_{12} \wedge \tau_{23} \wedge \tau_{31} \geq t] \propto t^{-\gamma(d)} \quad \text{as } t \rightarrow \infty, \quad (1.17)$$

where  $\gamma(d)$  is some critical exponent depending on the dimension. It is known that  $\gamma(1) = 3/2$ . It seems plausible that  $\gamma(d)$  is decreasing in  $d$  and that  $\gamma(d'_c) = 1$ , since this is the point where the expected time until two of three annihilating random walks annihilate each other becomes infinite, hence the branching becomes infinitely effective, in a sense. Unfortunately, we do not know the function  $\gamma(d)$ . A naive linear interpolation between  $\gamma(1) = 3/2$  and  $\gamma(2) = 0$  is consistent with a critical dimension  $d'_c = 4/3$ , however.

Of course, from the mathematical point of view, there is a considerable ambiguity in how one defines noninteger dimensions, while field-theoretical renormalization group arguments are out of scope of present day rigorous methods. From the field-theoretical perspective, the existence of a second critical dimension leads to considerable difficulties, to which the authors of [HCDDM05] reacted by considering non-perturbative techniques.

Recently, some rigorous mathematical work has been carried out on models belonging to the PC universality class. The DBARW from (1.11) has been studied in [Sud90]. This model can be exactly solved, in a certain sense, but unfortunately the model is in the absorbing phase for all  $\alpha > 0$ , hence there is no ‘true’ phase transition. (Nevertheless, its solution has been used in papers such as [CT98] to draw conclusions that presumably hold for the whole PC universality class.) No solvable models seem to be known that exhibit a true phase transition. (The one-sided rebellious voter model may be such a model, but we have not solved it; our proposed explicit formulas are backed up by simulations but not by calculations.)

Strong impetus to the mathematical study of models from the PC universality class came from the paper of Neuhauser and Pacala [NP99], which proposes a variation on the  $d$ -dimensional range- $N$  voter model governed by a parameter  $\alpha$  similar to our models. (This paper also considers more general models, where the symmetry between ones and zeros is broken, which fall outside the scope of the present paper.) Their model is dual to a system of parity preserving branching-annihilating random walks. For  $d = 1, N = 1$ , up to a rescaling of time, this dual model is the DBARW; this implies that the model of Neuhauser and Pacala with  $d = 1, N = 1$  exhibits noncoexistence for all  $\alpha > 0$ . For  $N \geq 2$  and  $d = 1$ , their model is supposed to exhibit a nontrivial phase transition between coexistence and noncoexistence. For  $d = 2$ , their model is supposed to exhibit noncoexistence only for  $\alpha = 1$  while in dimensions  $d \geq 3$  noncoexistence holds for all  $\alpha$ , in line with the predictions made in [CT98].

Much of this lacks rigorous proof. First of all, it is not rigorously known that coexistence is a decreasing property in  $\alpha$ , or, in terms of the dual model, that increasing the branching rate leads to more particles in the system. Obvious as this may seem, finding a rigorous proof seems hard. Second, there exists no rigorous proof of noncoexistence (or equivalently, the existence of an absorbing phase for the dual model) except in the trivial cases  $\alpha = 1$  (pure voter) or  $d = 1, N = 1$  (related to DBARW). On the other hand, there exist a number of rigorous results proving coexistence (or equivalently, the existence of an active phase for the dual model). Neuhauser and Pacala proved that their model exhibits coexistence for  $\alpha$  sufficiently close to zero for all values of  $d$  and  $N$  except  $d = 1, N = 1$ . The analogue result for the rebellious voter model was proved in [SS08a, Theorem 4]; see also [BEM06] which proved a similar result for branching-annihilating random walks which allow for more particles at one site. In [CP06], it has been proved that the model of Neuhauser and Pacala exhibits coexistence in dimensions  $d \geq 3$  for  $\alpha$  sufficiently close to *one* (the case of intermediate  $\alpha$  is still open due to the lack of a proof of monotonicity in  $\alpha$ ). The analogue result in  $d = 2$  is proved in [CMP09].

## 2 Main results

In this and the next section, we present data obtained by numerical simulations of the rebellious voter model and its one-sided counterpart. One of our main results is that two important functions one the one-sided process seem to be given by explicit formulas (see (2.7) below). In spite of our efforts, we have found no theoretical explanation for this apparent fact, not have we been able to find explicit formulas for any other functions of our processes. For those interested, the data underlying our figures are available from the homepage of the first author.

### 2.1 Methods

In our simulations, we start the interface process  $Y$  of either the rebellious voter model or its one-sided counterpart with an odd number of ones on an interval of  $N$  sites with periodic boundary conditions. Note that in this case, because the number of ones is odd and because of the periodic boundary conditions, we can no longer represent  $Y$  as in (1.7), but the dynamics in (1.8) and (1.9), as well as the duality relation (1.12), still make sense. Since we start with one particle, because of parity conservation, the system cannot die out. Letting  $Y_\infty$  denote the process in equilibrium, we assume that for large  $N$ , the following approximations are valid:

$$\begin{aligned} \text{(i)} \quad \rho(\alpha) &\approx 2\mathbb{P}[Y_\infty(0) = 1] = \frac{2}{N}\mathbb{E}[|Y_\infty|], \\ \text{(ii)} \quad \chi(\alpha) &\approx \mathbb{P}[|Y_\infty| = 1]. \end{aligned} \tag{2.1}$$

The arguments why formula (2.1) (ii) should hold are obvious from (1.7) and (1.16). The justification of formula (2.1) (i) is more subtle. Let  $Y^{1/2}$  denote the interface process of the rebellious voter model on  $\mathbb{Z}$ , started in an initial law such that the  $(Y_0(i))_{i \in \mathbb{Z}}$  are independent with  $\mathbb{P}[Y_0(i) = 0] = \mathbb{P}[Y_0(i) = 1] = \frac{1}{2}$ , and let  $X$  be the rebellious voter model started in  $X_0 = \delta_0$ . Then by duality (1.12),

$$\mathbb{P}[Y_t^{1/2}(0) = 1] = \mathbb{P}[|Y_t^{1/2} X_0| \text{ is odd}] = \mathbb{P}[|Y_0^{1/2} X_t| \text{ is odd}] = \frac{1}{2}\mathbb{P}[X_t \neq \underline{0}], \tag{2.2}$$

where  $\underline{0}$  denotes the constant zero configuration. It is known that the law of  $Y_t^{1/2}$  converges as  $t \rightarrow \infty$  to an invariant law, which is in fact the unique spatially homogeneous, nontrivial

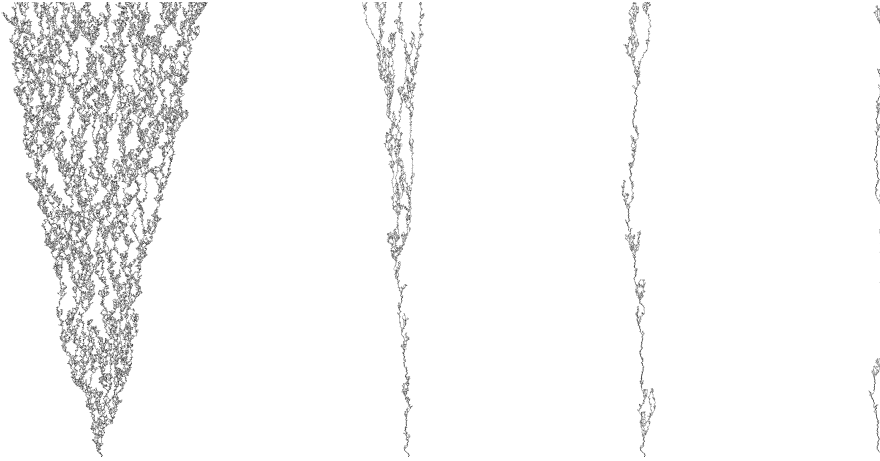


Figure 1: The interface model  $Y$  of the rebellious voter model for  $\alpha = 0.4$ ,  $\alpha = 0.5$ ,  $\alpha = 0.51$  and  $\alpha = 0.6$ , started with a single interface. Space is plotted horizontally and time vertically, with a black spot at a point  $(i, t)$  indicating that  $Y_t(i) = 1$ . Total time elapsed in each picture is 1800.

invariant of the process [SS08a, formula (1.12) and Theorem 3 (b)]. Taking the limit  $t \rightarrow \infty$  in (2.2), we see that for this invariant law, formula (2.1) (i) holds with equality. Since it seems reasonable that the invariant laws of our finite systems approximate the invariant law of the infinite system, this justifies (2.1) (i). Similar arguments apply to the one-sided model.

## 2.2 A first qualitative look

Before we present our numerical data for the functions  $\rho$  and  $\chi$  from (2.1), we first take a look at the qualitative behavior of the interface model  $Y$  of the rebellious voter model and its one-sided analogue. In Figure 1, we have graphically plotted  $Y$  for the two-sided process, started with a single one, with time running upwards and a black spot at a point  $(i, t)$  indicating that  $Y_t(i) = 1$ . The figures show the process for four values of  $\alpha$ , where  $\alpha_c \approx 0.51$  is the estimated critical value for this process (see Section 2.3 below).

The pictures show that for  $\alpha < \alpha_c$ , all ones are contained in an interval with edges that grow at an approximately linear speed, and that inside this interval, ones occur at some approximately constant equilibrium density. On the other hand, for  $\alpha > \alpha_c$ , the process spends a positive fraction of its time in states where there is just a single site in state one, which indicates that the rebellious voter model exhibits interface tightness (see (1.16)). What happens exactly at  $\alpha = \alpha_c$  is less clear from these pictures, but our numerical data, presented in Sections 2.3 and 3.3 below, suggest that at  $\alpha = \alpha_c$ , the edge speed is zero and the rebellious voter model exhibits neither coexistence nor interface tightness.

The picture for the one-sided process is very similar, except that now, due to the nature of the process, the process as a whole tends to drift to the right at some approximately constant speed; see Figure 2.

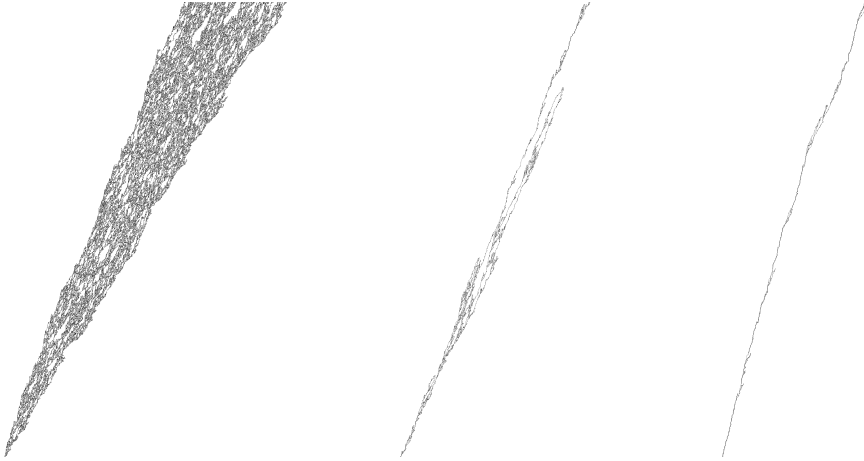


Figure 2: The interface model of the one-sided rebellious voter model for  $\alpha = 0.3$ ,  $\alpha = 0.5$  and  $\alpha = 0.6$ .

### 2.3 The two-sided model

We simulated the interface model  $Y$  of the rebellious voter model on an interval of  $N$  sites with periodic boundary conditions by slowly increasing or decreasing  $\alpha$  from some initial value  $\alpha_b$  to some final value  $\alpha_e$  during a time interval of length  $T$ . We then divided our time interval into  $n$  equal pieces and plotted the average value of  $2|Y|/N$  (for the function  $\rho$ ) or the fraction of the time that  $|Y| = 1$  (for the function  $\chi$ ) against the average value of  $\alpha$ , for each of the  $n$  time intervals. The resulting approximations for  $\rho$  and  $\chi$  for one such run are plotted in Figure 3. These data use the parameters:

$$\begin{aligned} \text{for } \rho: & \quad N = 2^{15}, n = 2^9, T = 10^8, \alpha_b = 0, \alpha_e = 0.55, \\ \text{for } \chi: & \quad N = 2^{15}, n = 2^9, T = 10^{12}, \alpha_b = 0.99, \alpha_e = 0.49. \end{aligned} \quad (2.3)$$

The values  $\rho(0) = 1$  and  $\chi(1) = 1$  are expected on theoretical grounds. Indeed, it is easy to check that the rebellious voter model with  $\alpha = 0$  never dies out (recall (1.14)) while in the pure voter case  $\alpha = 1$ , the process started in a Heaviside state stays in such a state for all time (recall (1.16)).

The numerical data for  $\rho$  are well fitted by a linear fractional function of the form

$$\rho(\alpha) = \frac{1 - c_1\alpha}{1 - c_2\alpha} \quad \text{with} \quad c_1 = 1.958 \pm 0.001 \quad \text{and} \quad c_2 = 0.975 \pm 0.002, \quad (2.4)$$

(see Figure 4). Assuming this sort of function fitting is justified, we arrive at an estimate for the critical point of

$$\alpha_c = 0.5107 \pm 0.0003. \quad (2.5)$$

This estimate is to be viewed with caution, since this is based on extrapolation of data for (approximately)  $0 \leq \alpha \leq 0.35$ , assuming that the linear fractional form (2.4) holds for all  $\alpha \leq \alpha_c$ . A more robust method (see Figure 5) based on our best data for the functions  $\rho$  and  $\chi$  near the critical point leads to the estimate:

$$\alpha_c = 0.510 \pm 0.002. \quad (2.6)$$

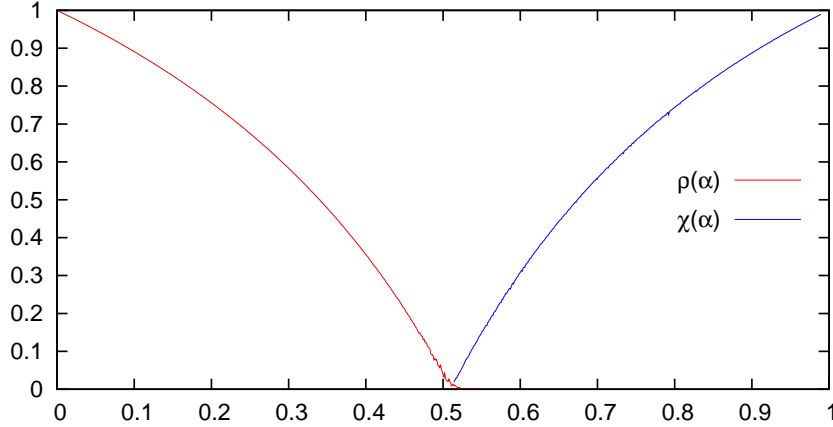


Figure 3: The functions  $\rho$  and  $\chi$  for the rebellious voter model. Data obtained with parameters as in (2.3).

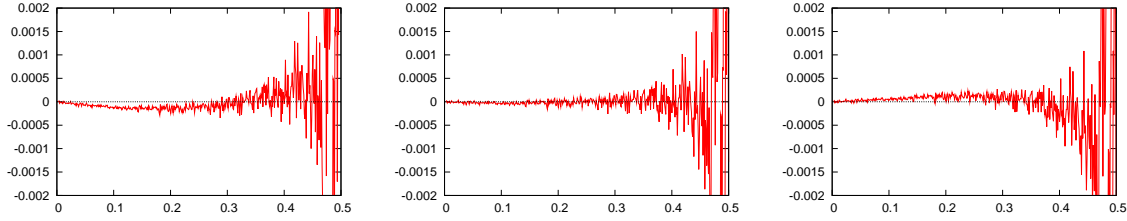


Figure 4: The function  $\rho(\alpha) - (1 - c_1\alpha)/(1 - c_2\alpha)$  for the values  $c_1 = 1.957$ ,  $c_2 = 0.973$  (left),  $c_1 = 1.958$ ,  $c_2 = 0.975$  (middle) and  $c_1 = 1.959$ ,  $c_2 = 0.977$  (right).

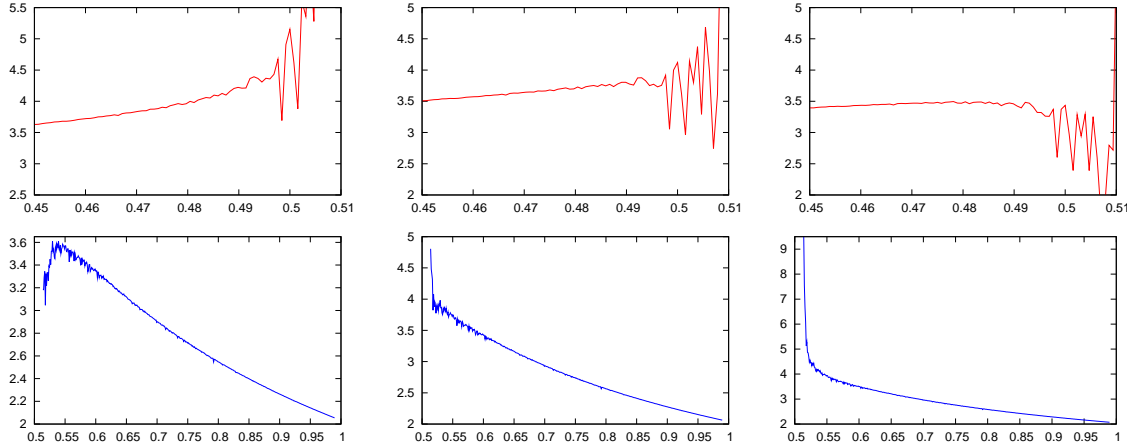


Figure 5: Estimation of the critical point of the rebellious voter model. Above: The function  $\rho(\alpha)/(\alpha_0 - \alpha)$  for the values  $\alpha_0 = 0.508$  (left),  $\alpha_0 = 0.510$  (middle) and  $\alpha_0 = 0.512$  (right). Below: the function  $\chi(\alpha)/(\alpha - \alpha_0)$  for the values  $\alpha_0 = 0.508$  (left),  $\alpha_0 = 0.510$  (middle) and  $\alpha_0 = 0.512$  (right). Our simulations for  $\rho$  use the parameters  $N = 2^{15}$ ,  $n = 2^7$ ,  $T = 10^9$ ,  $\alpha_b = 0.55$ ,  $\alpha_e = 0.45$  and those for  $\chi$  use the parameters in (2.3).

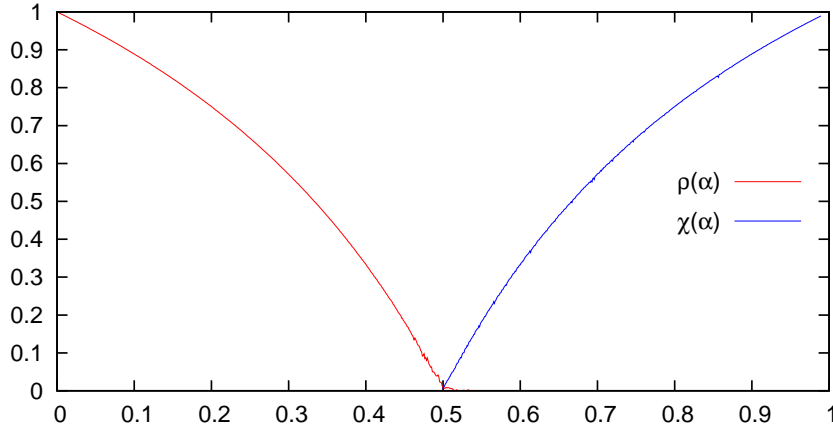


Figure 6: The functions  $\rho$  and  $\chi$  for the one-sided rebellious voter model. Data obtained with parameters as in (2.3).

(See also Figure 8.) It seems that linear fractional functions do not fit the numerical data for  $\chi$  really well.

Our data strongly suggest that  $\rho(\alpha_c) = 0 = \chi(\alpha_c)$ , which implies that at criticality, the process exhibits neither coexistence nor interface stability. Summarizing, the picture that emerges from our numerical data is as follows:

There exists a critical value  $\alpha_c \approx 0.510$  such that the rebellious voter model exhibits coexistence if and only if  $\alpha < \alpha_c$  and interface tightness if and only if  $\alpha > \alpha_c$ . The function  $\rho$  from (1.14) has a finite negative slope and is concave on  $[0, \alpha_c]$ , and is approximately given by a linear fractional function of the form (2.4). The function  $\chi$  from (1.16) has a finite positive slope and is concave on  $[\alpha_c, 1]$ .

## 2.4 The one-sided model

We have run the same simulation as described in the previous section, with parameters as in (2.3), also for the one-sided rebellious voter model. The resulting approximations for the functions  $\rho$  and  $\chi$  are plotted in Figure 6.

At first sight, Figure 6 looks extremely similar to Figure 3. A closer inspection reveals, however, that the two plots are not identical. Indeed, it seems that for the one-sided model, the functions  $\rho$  and  $\chi$  are described by the explicit formulas:

$$\rho(\alpha) = 0 \vee \frac{1 - 2\alpha}{1 - \alpha} \quad \text{and} \quad \chi(\alpha) = 0 \vee \left(2 - \frac{1}{\alpha}\right). \quad (2.7)$$

In particular, one has the symmetry  $\rho(1 - \alpha) = \chi(\alpha)$  and the critical parameter seems to be given by

$$\alpha_c = 0.500 \pm 0.002 = \frac{1}{2} \quad (?) \quad (2.8)$$

In Figure 7, we have plotted the differences between the explicit functions in (2.7) and our data for  $\rho$  and  $\chi$ , respectively. We have no idea why these explicit formulas should fit our numerical data so precisely. In fact, most hypothetical explanations that come to one's mind

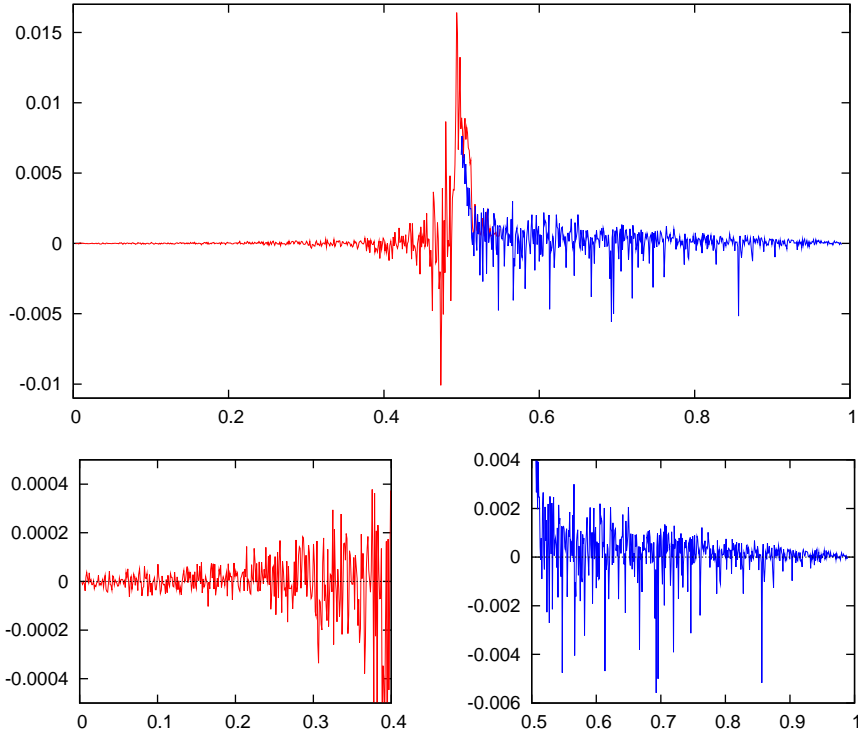


Figure 7: Difference between the explicit formulas in (2.7) and the functions  $\rho$  and  $\chi$  for the one-sided rebellious voter model, with detail of the left and right side of the picture.

should apply to the two-sided model as well, for which our numerical data convincingly show that the formulas in (2.7) do not fit. We have no idea why the one-sided model, which has less symmetry than the two-sided model, should be more tractable than the latter.<sup>1</sup> A detailed comparison of the two-sided and one-sided model near the critical point is shown in Figure 8.

## 2.5 Finite size effects

To gain more insight into how close our numerical data are to the real functions  $\rho$  and  $\chi$ , we tested the effect of varying the system size  $N$ . In Figure 9 we have plotted our approximation (see (2.1)) of the function  $\rho$  for different values of the system size  $N$ . The pictures for the two-sided and one-sided process are extremely similar, except for a shift of the critical point. In view of Figure 9, it seems that we can rule out the possibility that the observed differences between the two-sided and one-sided process are due to finite space effects (and a hypothetical slower convergence for the two-sided model).

Note that in Figure 9, our approximations to  $\rho$  near the critical point become more rough as the system size is increased. This can be understood due to two effects. On the one hand, near

<sup>1</sup>Perhaps the only aspect in which the one-sided model is potentially simpler than the two-sided model is that in the former, information is passed only from left to right. A third model, which we have only studied briefly, in which voter model updates look to the right and rebellious updates look to the left, seems to have a critical point  $\alpha_c = 0.510 \pm 0.003$  and functions  $\rho, \chi$  that are close, but not identical to those of the two-sided rebellious voter model.

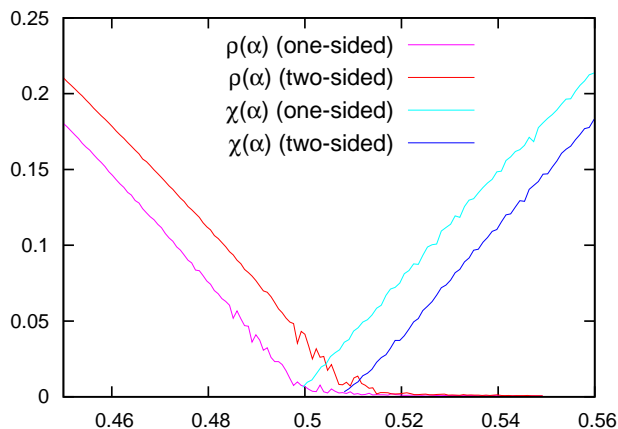


Figure 8: A detailed simulation near the critical point of the functions  $\rho$  and  $\chi$  for the two-sided process and the one-sided process. Our simulations for  $\rho$  use the parameters  $N = 2^{15}$ ,  $n = 2^7$ ,  $T = 10^9$ ,  $\alpha_b = 0.55$ ,  $\alpha_e = 0.45$ . Our plots for  $\chi$  show detail of a simulation with the parameters  $N = 2^{15}$ ,  $n = 2^9$ ,  $T = 10^{12}$ ,  $\alpha_b = 0.99$ ,  $\alpha_e = 0.5$ .

criticality, the random variable  $|Y_\infty|$  assumes the values  $1, 3, 5, 7, \dots$  with approximately equal probabilities (see Section 3.2), which means that the number of ones in the system fluctuates from being close to one to a positive fraction of all sites in the lattice. As the system size gets large, this means huge fluctuations, which are moreover slow since at criticality, the edge speed is zero.

In Figure 10, we have plotted our approximations for the function  $\chi$  for various values of  $N$ . To counteract the ‘roughening’ effect we have just described, in these simulations, we have increased the total time  $T$  together with the system size  $N$ . Again, the pictures for the two-sided and one-sided process are similar except for a small shift in the critical point.

We have also run simulations for different values of the total elapsed time, to investigate the effect of this parameter on the quality of our data. Since short times mean the system does not have enough time for time averages to reach their equilibrium values, the main effect of increasing  $T$  is to smoothen our approximated functions. For the function  $\rho$ , this effect is demonstrated in Figure 11. A second effect of choosing a too short time  $T$  is that the numerical functions ‘lag behind’ in that they show values belonging to an  $\alpha$  that lies somewhat in the past. This effect is demonstrated in Figure 12. In this case, our approximations near the critical point depend on the direction in which we vary  $\alpha$ : the graph produced by increasing  $\alpha$  ‘overshoots’ the critical point while the graph produced by lowering  $\alpha$  picks up too late. Also note the ‘hook’ at the beginning of the graph started with  $\alpha$  below the critical point, which is due to the fact that we start with a single one and the finite edge speed needs several time steps to fill out all space. This sort of effects only occur when  $T$  is small relative to  $N$ ; in all our simulations (except those in Figure 12) we have taken care to avoid such a choice of parameters.

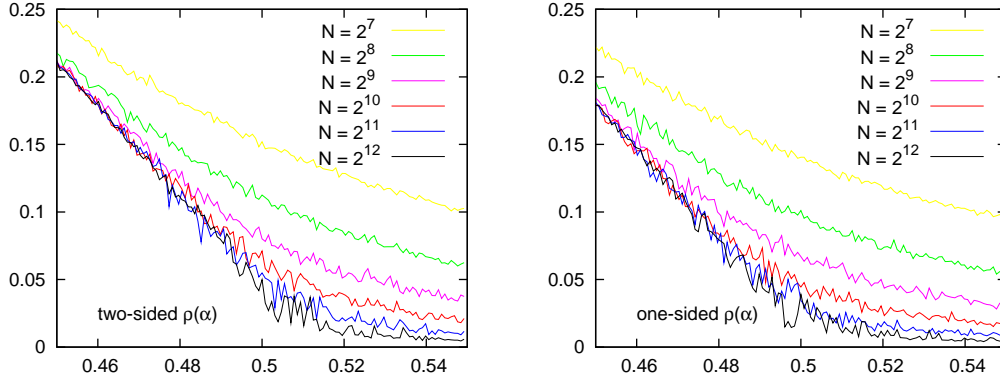


Figure 9: Effect of the system size on our approximation of the function  $\rho$  from (2.1). Plotted are our approximations for  $\rho$  using the parameters  $n = 2^7$ ,  $T = 10^8$ ,  $\alpha_b = 0.55$ ,  $\alpha_e = 0.45$ , and the system sizes  $N = 2^7, 2^8, 2^9, 2^{10}, 2^{11}, 2^{12}$ , respectively. On the left: the two-sided model. On the right: the one-sided model.

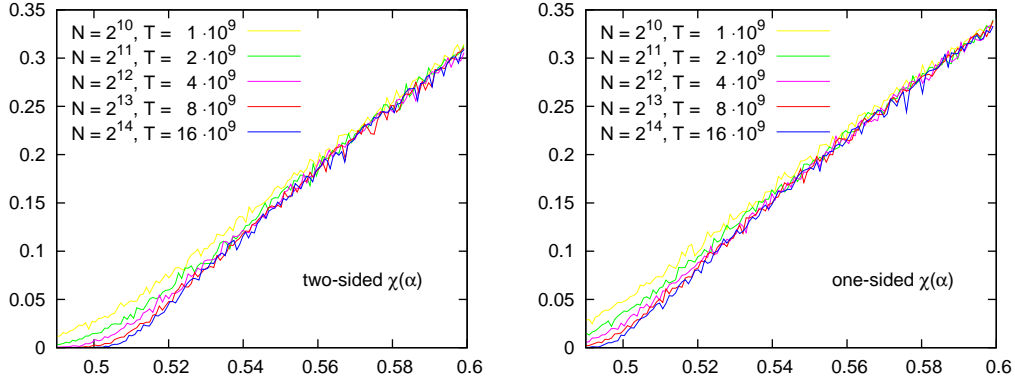


Figure 10: Effect of the system size on our approximation of the function  $\chi$  from (2.1). Plotted are our approximations for  $\chi$  using the parameters  $n = 2^7$ ,  $\alpha_b = 0.6$ ,  $\alpha_e = 0.49-0.5$ , and the system sizes  $N = 2^{10}, 2^{11}, 2^{12}, 2^{13}, 2^{14}$  and times  $T = 10^9, 2 \cdot 10^9, 4 \cdot 10^9, 8 \cdot 10^9, 16 \cdot 10^9$ , respectively. On the left: the two-sided model. On the right: the one-sided model.

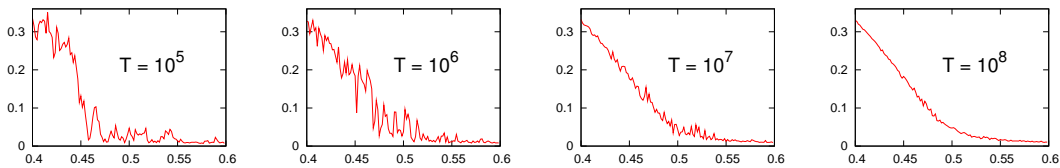


Figure 11: Effect of the duration of our simulations on our approximation of the function  $\rho$  from (2.1) for the one-sided model. Plotted are our approximations for  $\rho$  using the parameters  $N = 2^{10}$ ,  $n = 2^7$ ,  $\alpha_b = 0.6$ ,  $\alpha_e = 0.4$ , and the total elapsed times  $T = 10^5, 10^6, 10^7, 10^8$ , respectively.

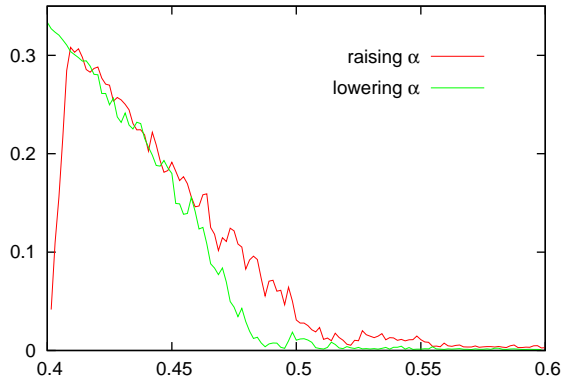


Figure 12: Effects of choosing the time too small compared to the system size, in simulations of  $\rho$  for the one-sided model. The blue curve was produced by raising  $\alpha$  from  $\alpha_b = 0.4$  to  $\alpha_e = 0.6$  while for the red curve we lowered  $\alpha$  from  $\alpha_b = 0.6$  to  $\alpha_e = 0.4$ . The other simulation parameters were  $n = 2^7$ ,  $N = 2^{13}$ , and  $T = 10^6$ .

### 3 Other functions of the process

#### 3.1 Harmonic functions

We have obtained numerical data for a number of other functions of our processes. We have mainly concentrated on the one-sided model, in view of the apparent explicit formulas for the functions  $\rho$  and  $\chi$  in this case. We have not been able, however, to find explicit formulas for any other functions than these two. Nevertheless, our additional functions show some interesting phenomena, which we discuss here. In the present section, we discuss a harmonic function for the (one-sided) rebellious voter model. In the next two sections, we look at the equilibrium probabilities of seeing 3, 5, 7, ... ones in the interface model, and edge speeds, respectively.

We first need to introduce some notation. In this section, we let  $X_t$  denote the rebellious voter model,  $\bar{X}_t$  the one-sided rebellious voter model, and  $\tilde{X}_t$  the mirror image of the latter, i.e., the model that jumps as

$$\begin{aligned}
 x \mapsto x^{\{i\}} \quad \text{with rate} \\
 \alpha 1_{\{x(i) \neq x(i+1)\}} + (1 - \alpha) 1_{\{x(i+1) \neq x(i+2)\}}.
 \end{aligned}
 \tag{3.1}$$

Let  $\tilde{Y}_t$  be the interface model of this mirrored one-sided rebellious voter model on an interval of  $N$  sites with periodic boundary conditions, started with an odd number of ones, and let  $\tilde{Y}_\infty$  denote the process in equilibrium. For each  $x \in \{0, 1\}^N$ , we define

$$\vec{f}_{x,N}(\alpha) := \frac{\mathbb{P}[|x\tilde{Y}_\infty| \text{ is odd}]}{\mathbb{P}[\tilde{Y}_\infty(0) \text{ is odd}]}.
 \tag{3.2}$$

(The reason for this notation with the vector on  $\vec{f}_{x,N}(\alpha)$  pointing to the right is that this is a harmonic function for the one-sided rebellious voter model  $\bar{X}$ , as explained below.)

We will mainly be interested in the case that  $x$  contains just a few ones close together. In view of this, we only write down only the part of  $x$  that is nonzero. For example, we

write  $\vec{f}_{1101,N}(\alpha)$  to denote the function  $\vec{f}_{x,N}(\alpha)$  where  $x$  is any element of  $\{0,1\}^N$  such that  $(x(i), x(i+1), x(i+2), x(i+3)) = (1, 1, 0, 1)$  for some  $i \in \{0, \dots, N-1\}$  and  $x(j) = 0$  for all  $j \neq i, i+1, i+2, i+3$ . Note that since the law of  $\vec{Y}_\infty$  is translation invariant (modulo  $N$ ), this definition does not depend on the value of  $i$ .

Using the fact that  $\vec{Y}_t$  is dual to  $\vec{X}_t$  in the sense of formula (1.12), it is not hard to show that  $\vec{f}_{x,N}(\alpha)$ , as a function of  $x$ , is a harmonic function for the one-sided rebellious voter model  $\vec{X}_t$  (on a finite interval with periodic boundary conditions), i.e., this is a function such that the process with competition parameter  $\alpha$  started in  $\vec{X}_0 = x$  satisfies  $E[\vec{f}_{\vec{X}_t,N}(\alpha)] = \vec{f}_{x,N}(\alpha)$  for all  $t \geq 0$ .

Our simulations suggest that the functions  $\vec{f}_{x,N}(\alpha)$  converge as  $N \rightarrow \infty$  to a nontrivial limit function  $\vec{f}_x(\alpha)$ , which is a harmonic function for the one-sided rebellious voter model  $\vec{X}_t$  on  $\mathbb{Z}$ , started with finitely many ones. If  $\alpha < \alpha_c$ , then on theoretical grounds one may expect that

$$\vec{f}_x(\alpha) = \frac{\vec{\rho}_x(\alpha)}{\vec{\rho}_1(\alpha)}, \quad \text{where} \quad \vec{\rho}_x(\alpha) := \mathbb{P}^x[\vec{X}_t \neq \underline{0} \ \forall t \geq 0] \quad (3.3)$$

denotes the probability that the one-sided rebellious voter model  $\vec{X}_t$  started in the initial state  $x$  survives. For  $\alpha > \alpha_c$ , it is less obvious how to interpret  $\vec{f}_x(\alpha)$ , but we still expect the limiting function to be harmonic. The fact that  $\vec{f}_x(\alpha)$  is harmonic means that  $\vec{G}\vec{f}_x(\alpha) = 0$ , where  $\vec{G}$  is the generator of the one-sided rebellious voter model, defined as

$$\vec{G}f_x := \sum_i (\alpha 1_{\{x(i-1) \neq x(i)\}} + (1-\alpha) 1_{\{x(i-2) \neq x(i-1)\}}) (f_{x^{(i)}} - f_x). \quad (3.4)$$

In particular, the facts that  $\vec{G}\vec{f}_1(\alpha) = 0$  and  $\vec{G}\vec{f}_{11}(\alpha) = 0$  lead to the relations

$$\begin{aligned} \alpha(\vec{f}_\emptyset(\alpha) - \vec{f}_1(\alpha)) + (\vec{f}_{11}(\alpha) - \vec{f}_1(\alpha)) + (1-\alpha)(\vec{f}_{101}(\alpha) - \vec{f}_1(\alpha)) &= 0, \\ \alpha(\vec{f}_{111}(\alpha) - \vec{f}_{11}(\alpha)) + (\vec{f}_1(\alpha) - \vec{f}_{11}(\alpha)) + (1-\alpha)(\vec{f}_{1101}(\alpha) - \vec{f}_{11}(\alpha)) &= 0, \end{aligned} \quad (3.5)$$

where  $\vec{f}_\emptyset(\alpha) = 0$  and  $\vec{f}_1(\alpha) = 1$ . An inspection of our numerical data shows that these equations are satisfied within the precision of our simulations.

Our numerical data for the functions  $\vec{f}_x(\alpha)$ , for some simple choices of the pattern  $x$ , are shown in Figure 13. Note that  $\vec{f}_1(x)$  (not shown in the figure) is by definition identically one, because of the normalization chosen in (3.2). A surprising fact is that the functions  $\vec{f}_x(\alpha)$  and their derivatives (shown in Figure 14) appear to continue smoothly across the critical point. Note that the normalization in (3.2) is crucial here, since above  $\alpha_c$ , both the numerator and the denominator tend to zero as  $N \rightarrow \infty$ . For  $\alpha = 1$  one has  $\vec{f}_x(\alpha) = |x|$ , which is a well-known harmonic function for the pure voter model. For  $\alpha = 0$ , one has  $\vec{f}_x(\alpha) = 1$  for all nonzero  $x$ , reflecting the fact that the process with  $\alpha = 0$  never dies out.

A few regularities may be observed from Figures 13 and 14. Let

$$x_n := \underbrace{11111111}_{n \text{ ones}} \quad \text{and} \quad x'_n := \underbrace{10000001}_{n-2 \text{ zeros}}. \quad (3.6)$$

One expects that for  $\alpha < \alpha_c$ ,

$$\lim_{n \rightarrow \infty} \vec{\rho}_{x_n}(\alpha) = 1 \quad \text{and} \quad \lim_{n \rightarrow \infty} \vec{\rho}_{x'_n}(\alpha) = 1 - (1 - \vec{\rho}_1(\alpha))^2. \quad (3.7)$$

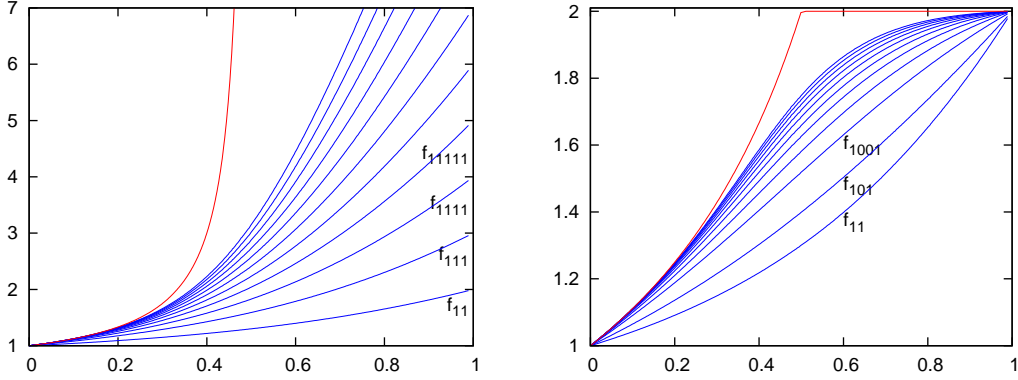


Figure 13: The functions  $\vec{f}_{11}, \vec{f}_{111}, \vec{f}_{1111}, \dots$  (left) and  $\vec{f}_{11}, \vec{f}_{101}, \vec{f}_{1001}, \dots$  (right). The functions in the left figure increase to the limit  $1/\rho(\alpha)$  while the functions in the right figure increase to  $2 - \rho(\alpha)$ . Both limits (theoretical curves) are plotted together with the data. The functions  $\vec{f}_{11}, \vec{f}_{111}, \vec{f}_{101}$  are based on data obtained with the parameters  $N = 2^{11}, n = 2^8, T = 10^8, \alpha_b = 0, \alpha_e = 0.5$  (left half of the pictures) and  $N = 2^{15}, n = 2^8, T = 10^9, \alpha_b = 0.99, \alpha_e = 0.51$  (right half of the pictures). The other functions are a combination of simulations using the parameters  $N = 2^{11}, n = 2^8, T = 10^8, \alpha_b = 0, \alpha_e = 0.5$  and  $N = 2^{15}, n = 2^8, T = 10^{10}, \alpha_b = 0.99, \alpha_e = 0.51$ .

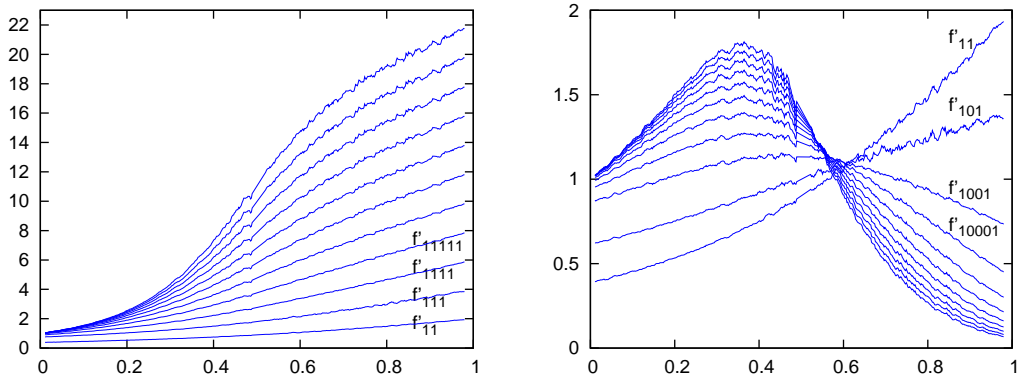


Figure 14: Derivatives of the functions from Figure 13. On the left  $\frac{\partial}{\partial \alpha} \vec{f}_{11}(\alpha), \frac{\partial}{\partial \alpha} \vec{f}_{111}(\alpha), \dots$ . On the right  $\frac{\partial}{\partial \alpha} f_{11}(\alpha), \frac{\partial}{\partial \alpha} f_{101}(\alpha), \frac{\partial}{\partial \alpha} f_{1001}(\alpha), \dots$ . Figure based on the same data as Figure 13. The derivatives are estimated with a quadratic Savitzky-Golay filter using 11 data points.

Hence, in view of (3.3), one expects that

$$\lim_{n \rightarrow \infty} \vec{f}_{x_n}(\alpha) = \vec{\rho}_1(\alpha)^{-1} \quad \text{and} \quad \lim_{n \rightarrow \infty} \vec{f}'_{x'_n}(\alpha) = 2 - \vec{\rho}_1(\alpha), \quad (3.8)$$

which is indeed what we observe.

From Figure 14 we moreover observe that

$$\left. \frac{\partial}{\partial \alpha} \vec{f}_{x_n}(\alpha) \right|_{\alpha=1} = 2(n-1) \quad (n \geq 2). \quad (3.9)$$

This can be explained on theoretical grounds. Indeed, if we write  $\vec{G} = \alpha \vec{G}_{\text{vot}} + (1-\alpha) \vec{G}_{\text{reb}}$ , where  $\vec{G}_{\text{vot}}$  and  $\vec{G}_{\text{reb}}$  are the (one-sided) voter and rebellious parts of the generator, then a simple calculation shows that

$$\vec{G}_{\text{vot}} \left. \frac{\partial}{\partial \alpha} \vec{f}_x(\alpha) \right|_{\alpha=1} = \vec{G}_{\text{reb}} \vec{f}_x(1). \quad (3.10)$$

Setting  $g_x := \left. \frac{\partial}{\partial \alpha} \vec{f}_x(\alpha) \right|_{\alpha=1}$ , this yields

$$\begin{aligned} g_{11} + g_{\emptyset} - 2g_1 &= \vec{G}_{\text{vot}} g_1 = \vec{G}_{\text{reb}} \vec{f}_1(1) = 2, \\ g_{111} + g_1 - 2g_{11} &= \vec{G}_{\text{vot}} g_{11} = \vec{G}_{\text{reb}} \vec{f}_{11}(1) = 0, \\ g_{1111} + g_{11} - 2g_{111} &= \vec{G}_{\text{vot}} g_{111} = \vec{G}_{\text{reb}} \vec{f}_{111}(1) = 0, \\ &\text{etcetera} \end{aligned} \quad (3.11)$$

Since  $f_{\emptyset}(\alpha) = 0$  and  $f_1(\alpha) = 1$  we have  $g_{\emptyset} = g_1 = 0$  and we can solve  $g_x$  inductively for  $x = 11, 111, 1111, \dots$  from (3.11).

The fact that the critical point and various other functions of the invariant law are different for the one-sided and two-sided model implies that the law of  $\vec{Y}_{\infty}$  cannot be mirror symmetric. Indeed, we observe that the functions  $f_{1011}(\alpha)$  and  $f_{1101}(\alpha)$  are not identical, as show in Figure 15.

### 3.2 Frequencies for three and more particles

As in the previous section, letting  $\vec{Y}_{\infty}$  denote the equilibrium interface process for the one-sided rebellious voter model, we have plotted in Figure 16 (picture on top left) the functions

$$\chi_k(\alpha) = \mathbb{P}[|\vec{Y}_{\infty}| = k] \quad (k = 1, 3, 5, \dots). \quad (3.12)$$

In particular,  $\chi_1$  is the function  $\chi$  from (2.1) (ii). Except for the case  $k = 1$  (see (2.7)), we have not found any simple explicit formulas that fit these curves. Nevertheless, some regularities may be noted. In particular, if we define

$$\theta_k(\alpha) := \frac{\chi_{k+2}(\alpha)}{\chi_k(\alpha)} \quad \text{and} \quad \phi_k(\alpha) := \frac{\theta_{k+2}(\alpha)}{\theta_k(\alpha)} \quad (k = 1, 3, 5, \dots), \quad (3.13)$$

then it seems that the functions  $\theta_k$  converge very fast to a limiting function  $\theta_{\infty}(\alpha) := \lim_{k \rightarrow \infty} \theta_k(\alpha)$ . (See Figure 16 picture on top right; the functions  $\theta_3, \theta_5, \dots$  all seem to fall on top of each other.) Likewise, the functions  $\phi_k$  converge very fast to the function that is identically one. (See Figure 16, two bottom pictures.) It is hard to obtain sufficiently precise data, but our best data (shown here) suggest that the function  $\phi_3$  is not identically one, although it is close. This means that the functions  $\theta_3$  and  $\theta_5$  are probably not identical, even

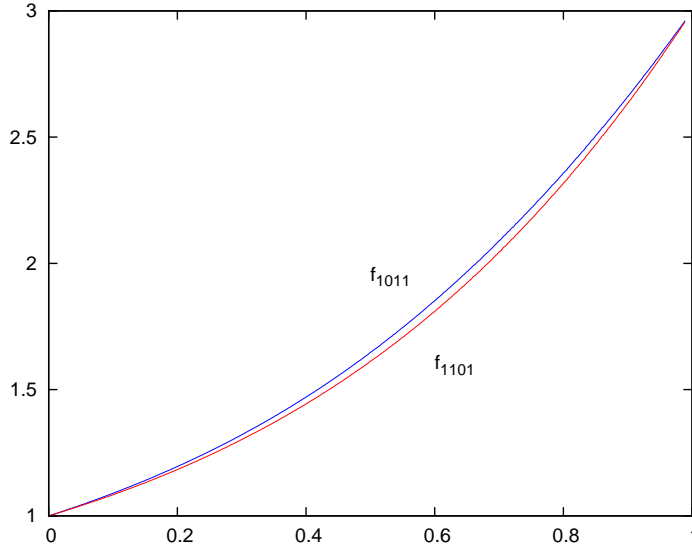


Figure 15: The functions  $f_{1011}$  and  $f_{1101}$  for the one-sided model, demonstrating the asymmetry of  $\vec{Y}_\infty$ . Combination of data obtained with the parameters  $N = 2^{11}$ ,  $n = 2^8$ ,  $T = 10^8$ ,  $\alpha_b = 0$ ,  $\alpha_e = 0.5$  and  $N = 2^{15}$ ,  $n = 2^8$ ,  $T = 10^9$ ,  $\alpha_b = 0.99$ ,  $\alpha_e = 0.51$ .

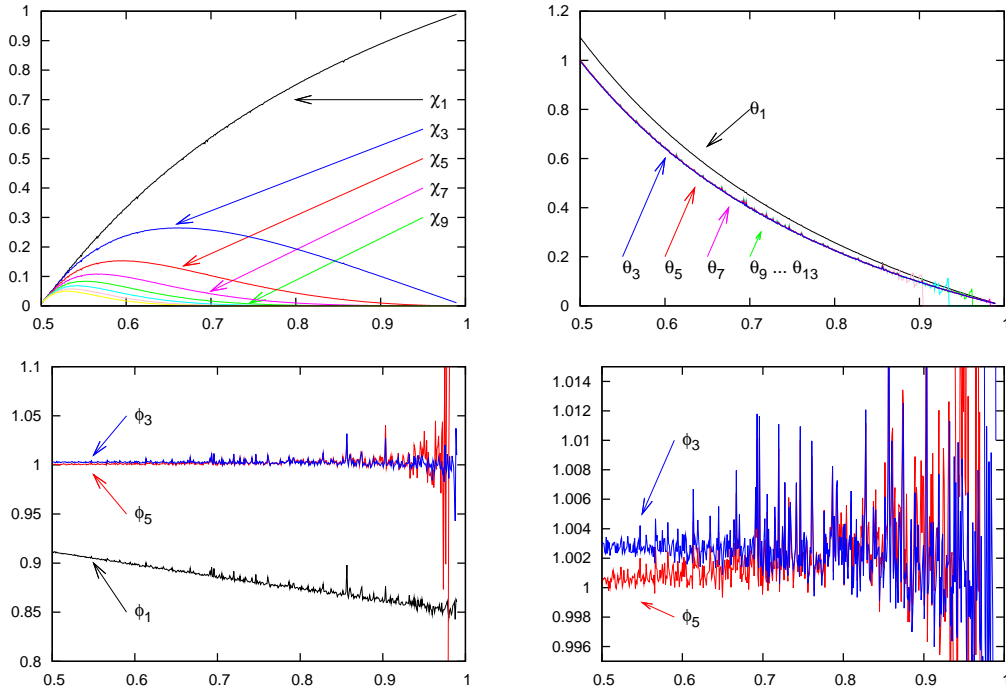


Figure 16: The frequency  $\chi_k(\alpha) = \mathbb{P}[|Y_\infty| = k]$  of seeing  $k$  particles for  $k = 1, 3, 5, \dots$  in the one-sided model. The second and third plot show the functions  $\theta_k(\alpha) := \chi_{k+2}(\alpha)/\chi_k(\alpha)$  and  $\phi_k(\alpha) := \theta_{k+2}(\alpha)/\theta_k(\alpha)$  for the first few values of  $k = 1, 3, 5, \dots$ . The fourth plot shows detail of the third plot. Data obtained with the parameters for  $\chi$  listed in (2.3)

though they almost fit each other in the picture on top right. Our numerical data are well fitted by the linear/constant functions:

$$\begin{aligned} \phi_1(\alpha) &\approx c_0 + c_1(\alpha - \tfrac{1}{2}) \quad \text{with} \quad c_0 = 0.9115 \pm 0.0015 \quad \text{and} \quad c_1 = -0.13 \pm 0.01, \\ \phi_3(\alpha) &\approx 1.0027 \pm 0.0005. \end{aligned} \tag{3.14}$$

and  $\phi_k(\alpha) = 1$  for  $k \geq 5$ . We note that if one assumes that the explicit formula for  $\chi_1(\alpha)$  in (2.7) is correct, and one knows the functions  $\phi_k(\alpha)$  for each  $k = 1, 3, \dots$ , then using the fact that  $\sum_{n=0}^{\infty} \chi_{2n+1}(\alpha) = 1$  one has enough equations to solve the functions  $\chi_k(\alpha)$  for each  $k = 1, 3, \dots$ .

The limiting function  $\theta_{\infty}(\alpha) := \lim_{k \rightarrow \infty} \theta_k(\alpha)$  seems to be strictly decreasing and concave on  $[\frac{1}{2}, 1]$  and satisfy  $\theta(\frac{1}{2}) = 1$ ,  $\theta(1) = 0$ . This implies that the distribution of the number of particles in equilibrium has an exponentially decaying tail for each  $\alpha > \frac{1}{2}$ . In particular, the mean number of particles

$$\mu(\alpha) := \mathbb{E}[|Y_{\infty}|] \tag{3.15}$$

is finite for all  $\alpha > \frac{1}{2}$  and diverges as  $\alpha \downarrow \frac{1}{2}$ .

The picture for the (two-sided) rebellious voter model is extremely similar, except that the critical point is no longer 0.5 and we have no explicit formula for  $\chi_1(\alpha)$ .

### 3.3 Edge speeds

Let  $Y_t$  be the interface model of the (two- or one-sided) rebellious voter model started with a finite number of ones and let

$$l_t := \inf\{i \in \mathbb{Z} : Y_t(i) = 1\} \quad \text{and} \quad r_t := \sup\{i \in \mathbb{Z} : Y_t(i) = 1\} \tag{3.16}$$

denote the position of the left-most and right-most ones, respectively. Our simulations suggest that there exist constants  $v_-(\alpha) \leq v_+(\alpha)$ , called the *left* and *right edge speed*, respectively, such that

$$\lim_{t \rightarrow \infty} \frac{l_t}{t} = v_-(\alpha) \quad \text{and} \quad \lim_{t \rightarrow \infty} \frac{r_t}{t} = v_+(\alpha) \quad \text{a.s.} \tag{3.17}$$

Set

$$Z_t(i) := Y_t(l_t + i) \quad (i \geq 0, t \geq 0). \tag{3.18}$$

Then  $Z_t$  describes the process  $Y_t$  as seen from the left-most one. It seems reasonable to assume that the law of  $Z_t$  converges as  $t \rightarrow \infty$  to some equilibrium law. Let  $Z_{\infty}$  denote the process in equilibrium. The left edge speed  $v_-(\alpha)$  can be obtained as the equilibrium expectation  $\mathbb{E}[f(Z_{\infty})]$  of a suitable function  $f$  which sums the sizes of all possible changes of  $l_t$  multiplied with the rate at which they occur.

We have simulated the process  $Z_t$  on a finite interval of  $N$  sites by neglecting all particles that fall off the right edge of the interval due to the dynamics of  $Y_t$  or the shifts in  $l_t$ . This process does not preserve parity, but if  $N$  is large enough the probability that all particles annihilate each other is very small. For most of our data points, such events never occurred, and when they occurred (especially near the critical point) they were so rare that they likely had no big influence on our estimate of the speeds. By slowly lowering or raising  $\alpha$  in our usual fashion and keeping track of all changes in  $Z_t$  that correspond to a change in  $l_t$  we obtained numerical data for the left edge speed  $v_-(\alpha)$  and, in a similar fashion, also for the right edge speed  $v_+(\alpha)$ , both for the two-sided and one-sided model.

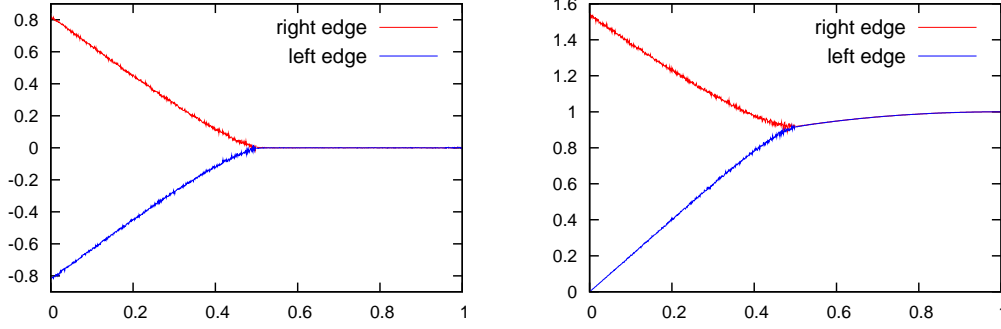


Figure 17: Edge speeds for the rebellious voter model (left) and its one-sided counterpart (right). The pictures show the speed of the right edge and left edge as a function of  $\alpha$ . Parameters used are  $N = 2^{11}$ ,  $n = 2^9$ ,  $T = 10^9$ ,  $\alpha_b = 0$ ,  $\alpha_e = 0.5$  (left half of each picture) and  $N = 2^{11}$ ,  $n = 2^9$ ,  $T = 10^{11}$ ,  $\alpha_b = 0.999$ ,  $\alpha_e = 0.5$  (right half of each picture).

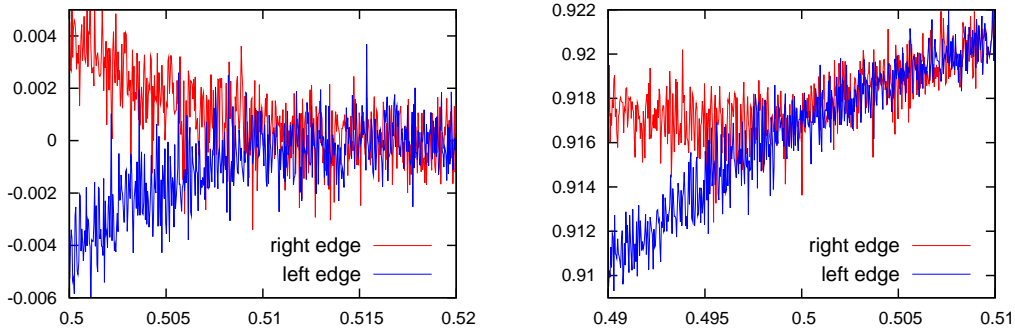


Figure 18: Detail of Figure 17. Parameters used are  $N = 2^{15}$ ,  $n = 2^9$ ,  $T = 10^{11}$ , with  $\alpha_b = 0.52$ ,  $\alpha_e = 0.5$  for the two-sided model and  $\alpha_b = 0.51$ ,  $\alpha_e = 0.49$  for the one-sided model. The curves have been smoothed a bit, corresponding to (effectively)  $n = 2^9/3$ .

The results are shown in Figure 17. One has  $v_-(\alpha) < v_+(\alpha)$  if and only if  $\alpha < \alpha_c$  and the functions  $v_-(\alpha)$  and  $v_+(\alpha)$  are strictly increasing resp. decreasing on  $[0, \alpha_c)$ . For the two-sided model, by symmetry,  $v_-(\alpha) = -v_+(\alpha)$  and hence  $v_-(\alpha) = 0 = v_+(\alpha)$  for  $\alpha \geq \alpha_c$ , while for the one-sided model one has  $0 \leq v_-(\alpha)$ , but otherwise the two pictures are remarkably similar. A detailed simulation near the critical point (shown in Figure 18) shows that the estimates for the critical points which one obtains from these simulations are consistent with our earlier estimates. Apart from the obvious values  $v_-(0) = 0$  and  $v_-(1) = v_+(1) = 1$  (for the one-sided model) and  $v_-(1) = v_+(1) = 0$  (for the two-sided model) we are not able to say anything explicit about the curves  $v_-(\alpha)$  and  $v_+(\alpha)$ .

## References

[BEM06] J. Blath, A. Etheridge, and M. Meredith. Coexistence in locally regulated competing populations and survival of branching annihilating random walk. *Ann.*

- Appl. Probab.* 17(5-6), 1474–1507, 2007.
- [CD95] J.T. Cox and R. Durrett. Hybrid zones and voter model interfaces. *Bernoulli* 1(4): 343–370, 1995.
- [CMP09] J.T. Cox, M. Merle, and E.A. Perkins. Co-existence in a two-dimensional Lotka-Volterra model. Preprint, 2009.
- [CP06] J.T. Cox and E.A. Perkins. Survival and coexistence in stochastic spatial Lotka-Volterra models. *Probab. Theory Relat. Fields* 139(1-2), 89–142, 2007.
- [CS73] P. Clifford and A. Sudbury. A model for spatial conflict. *Biometrika* 60, 581–588, 1973.
- [CT98] J.L. Cardy and U.C. Täuber. Field theory of branching and annihilating random walks. *J. Stat. Phys.* 90, 1–56, 1998.
- [GKT84] P. Grassberger, F. Krause and T. von der Twer. A new type of kinetic critical phenomenon *J. Phys. A: Math. Gen.* 17, 105–109, 1984.
- [Gri79] D. Griffeath. *Additive and Cancellative Interacting Particle Systems*. Lecture Notes in Math. 724, Springer, Berlin, 1979.
- [HCDDM05] O. Al Hammal, H. Chaté, B. Delmotte, I. Dornic, and M.A. Muñoz. Nonperturbative fixed point in a nonequilibrium phase transition. *Phys. Rev. Lett.* 95(10), 100601, 2005.
- [Hin00] H. Hinrichsen. Nonequilibrium critical phenomena and phase transitions into absorbing states. *Adv. Phys.* 49(7), 815–958, 2000.
- [HL75] R. Holley and T.M. Liggett. Ergodic theorems for weakly interacting systems and the voter model. *Ann. Probab.* 3, 643–663, 1975.
- [IT98] N. Inui and A.Yu. Tretyakov. Critical behavior of the contact process with parity conservation. *Phys. Rev. Lett.* 80(23), 5148–5151, 1998.
- [Jen94] I. Jensen. Critical exponents for branching annihilating random walks with an even number of offspring. *Phys. Rev. E* 50(5), 3623–3633, 1994.
- [NP99] C. Neuhauser and S.W. Pacala. An explicitly spatial version of the Lotka-Volterra model with interspecific competition. *Ann. Appl. Probab.* 9(4): 1226–1259, 1999.
- [OS05] G. Ódor and A. Szolnoki. Cluster mean field study of the parity-conserving phase transition. *Phys. Rev. E* 71(6), 066128, 2005.
- [SS08a] A. Sturm and J.M. Swart. Voter models with heterozygosity selection. *Ann. Appl. Probab.* 18(1), 59–99, 2008.
- [SS08b] A. Sturm and J.M. Swart. Tightness of voter model interfaces. *Electron. Commun. Probab.* 13, paper No. 16, 165–174, 2008.
- [Sud90] A. Sudbury. The branching annihilating process: an interacting particle system. *Ann. Probab.* 18: 581–601, 1990.

- [TT92] H. Takayasu and A.Yu. Tretyakov. Extinction, survival, and dynamical phase transition of branching annihilating random walk. *Phys. Rev. Lett.* 68(20), 3060–3063, 1992.